Unexpected magnetism of small silver clusters

M. Pereiro,[1,2,*] D. Baldomir,[1,2] and J. E. Arias[2]
[1]*Departamento de Física Aplicada, Universidade de Santiago de Compostela, Santiago de Compostela E-15782, Spain*
[2]*Instituto de Investigacións Tecnolóxicas, Universidade de Santiago de Compostela, Santiago de Compostela E-15782, Spain*
(Received 9 April 2007; published 26 June 2007)

The ground-state electronic and magnetic properties of small silver clusters Ag_n $(2 \leqslant n \leqslant 22)$ have been studied using a linear combination of atomic Gaussian-type orbitals within the density functional theory. The results show that the silver atoms, which are diamagnetic in a bulk environment, can be magnetic when they are grouped together in clusters. The Ag_{13} cluster with icosahedral symmetry has the highest magnetic moment per atom among the silver clusters studied. The cluster symmetry and the reduced coordination number specific to small clusters are revealed as a fundamental factor for the onset of magnetism.

DOI: 10.1103/PhysRevA.75.063204 PACS number(s): 36.40.Cg, 31.15.Ar, 36.40.Qv

I. INTRODUCTION

In the last two decades, the research field of clusters has shown rapid development in both experimental and theoretical investigations [1], since the clusters are well suited for several applications. For example, there has been a traditional interest in applications to catalysis [2], due to the considerable surface to volume ratio of clusters. More recently, clusters or nanoparticles that possess magnetic properties have offered exciting new opportunities for biomedical applications including (i) magnetic separation of labeled cells; (ii) therapeutic drug delivery; (iii) hyperthermic treatment for malignant cells; (iv) contrast enhancement agents for magnetic resonance imaging applications; and (v) also very recently for manipulating cell membranes [3].

Clusters are on the borderline between atoms and bulk, and thereby they play an important role in understanding the transition from the microscopic structure to the macroscopic structure of matter. Although $4d$ and $5d$ transition metal atoms have unfilled localized d states, none of them are magnetic. Only a few of the $3d$ transition metals form magnetic solids. Thus, from the magnetic point of view, one of the long-standing problems in condensed matter physics is to understand why some nonmagnetic metals become magnetic when they condense into clusters. There are two factors characteristic of clusters that mainly contribute to the onset and enhancement of the magnetism, namely, the reduced coordination number and the high symmetry, since symmetry enables degeneracy and degeneracy spawns magnetism [4–6]. According to this, an icosahedral structure is a good candidate for the appearance of the magnetism because the maximal degeneracy of an irreducible representation of the icosahedra (I_h) group is 5 whereas all other cluster symmetries allow at most threefold degeneracy, as was reported by Reddy *et al.* for Pd, Rh, and Ru [7].

In this paper, we present first-principles calculations on small silver clusters exhibiting an important magnetism, which has not been predicted until now. In the present work we study the evolution of the magnetism of silver clusters as a function of the cluster size and special emphasis is placed on the effects of cluster symmetry. We show that some of the studied clusters exhibit magnetic behavior which is not present in bulk silver. To the best of our knowledge, nobody has predicted or observed magnetism in small bare silver clusters; however, our computational simulations anticipate the onset and enhancement of magnetism for the silver clusters that include special conditions like high symmetry and reduced coordination number. In this respect, the Ag_{13} cluster exhibits the highest magnetic moment among the studied clusters and converges into a stable structure.

II. METHOD

With the aim of studying the magnetic properties of small silver clusters Ag_n $(2 \leqslant n \leqslant 22)$, we have performed density-functional-theory-based calculations consisting of a linear combination of Gaussian-type-orbitals Kohn-Sham density-functional methodology as implemented in the DEMON-KS3P5 program package [8]. All-electron spin-unrestricted calculations were carried out at the generalized gradient approximation (GGA) level to take the exchange-correlation (XC) effects into account [9]. Local-density approximation sometimes yields inaccurate bond lengths and total energies due to the insufficiency in describing the strong correlation effect of the localized d electrons and charge density inhomogeneities. In these regards, the GGA should be a better choice [10]. For this reason, at the beginning of this work and to satisfy ourselves that the numerical procedure is reliable, we initiate a search for a functional that better fitted the calculated bond length of the silver dimer to the experimental one. We found that the functional that better fitted the bond length was the one developed by Perdew and Wang [9], giving a bond length of 2.535 Å, which is in excellent agreement with the experimental measure (2.533 50 Å) reported in Ref. [11]. An orbital basis set of contraction pattern (633321/53211*/531+) was used in conjunction with the corresponding (5,5;5,5) auxiliary basis set for describing the s, p, and d orbitals [12]. The grid for numerical evaluation of the XC terms had 128 radial shells of points and each shell had 26 angular points. Spurious one-center contributions to the XC forces, typically found in systems with metal-metalbonds when using a nonlocal functional, are eliminated in a similar way as has been done in Ref. [13]. The geometries were fully optimized without symmetry and geometry constraints using the Broyden-Fletcher-Goldfarb-Shanno al-

*Corresponding author. fampl@usc.es

 ©2007 The American Physical Society

TABLE I. Energy differences between various spin states relative to the most stable spin configuration. The energy is given in units of eV/atom and M is the spin multiplicity.

Even-numbered clusters							Odd-numbered clusters						
		M							M				
Cluster	Symmetry	1	3	5	7	9	Cluster	Symmetry	2	4	6	8	10
Ag_2	$D_{\infty h}$	0.00	0.72	4.28			Ag_3	C_{2v}	0.00	0.67	2.83		
Ag_4	D_{2h}	0.00	0.16	1.19			Ag_5	C_{2v}	0.00	0.35	1.27		
Ag_6	D_{3h}	0.00	0.37	0.76			Ag_7	D_{5h}	0.00	0.30	0.66		
Ag_8	D_{2d}	0.00	0.28	0.52			Ag_9	C_s	0.00	0.27	0.45		
Ag_{10}	D_{2d}	0.00	0.18	0.40			Ag_{11}	C_1	0.00	0.20	0.34		
Ag_{12}	C_s	0.00	0.16	0.27			Ag_{13}	I_h	0.24	0.23	0.00	0.44	0.80
Ag_{14}	C_{3v}	0.52	0.50	0.00	0.09	0.82	Ag_{15}	C_{2v}	0.49	0.00	0.06		
Ag_{16}	C_s	0.49	0.00	0.04	0.16		Ag_{17}	C_2	0.00	0.03	0.62	0.24	
Ag_{18}	C_s	0.00	0.03	0.08	0.18		Ag_{19}	D_{5h}	0.00	0.02	0.07	0.67	
Ag_{20}	C_{2v}	0.01	0.00	0.05	0.13		Ag_{21}	C_1	0.00	0.02	0.08	0.16	
Ag_{22}	C_s	0.50	0.00	0.02	0.07								

gorithm [14]. During the optimization, the convergence criterion for the norm of the energy gradient was fixed to 10^{-4} a.u., while it was 10^{-7} a.u. for the energy and 10^{-6} a.u. for the charge density. A wide set of spin multiplicities ranging from 1 up to a maximum of 10, depending on the cluster size, was checked to ensure that the lowest-energy electronic and magnetic configuration is reached. In Table I, we collect the energy difference for several spin states. We observe that the majority of the clusters are very stable from the magnetic point of view, since the energy difference of the excited spin states relative to the most stable spin configuration is greater than 24 meV/atom $\approx$ 273 K/atom. The only exception to this behavior occurs for clusters with size varying from $n=19$ up to 22 (Ag_{19}–Ag_{22}), which can be better described as "magnetically fluxional."

A huge sampling of trial geometries taken from the literature was evaluated. While for these small clusters it is nearly impossible to search for all possible geometries, the detailed search that we have carried out gives us some confidence that the structural minimum has been found. A detailed study about the structural stability and the static response properties of these small silver clusters has been published in Ref. [15]. Consequently, the ground-state structures of Ag_n ($n=2$–22) employed in this study and plotted in Fig. 1 are those of Ref. [15]. It is worthwhile to mention the fact that other authors did not find the icosahedron as the global minimum of Ag_{13} and, in consequence, the magnetic properties of Ag_{13} and even Ag_{14} predicted by us could differ from those in other work [16].

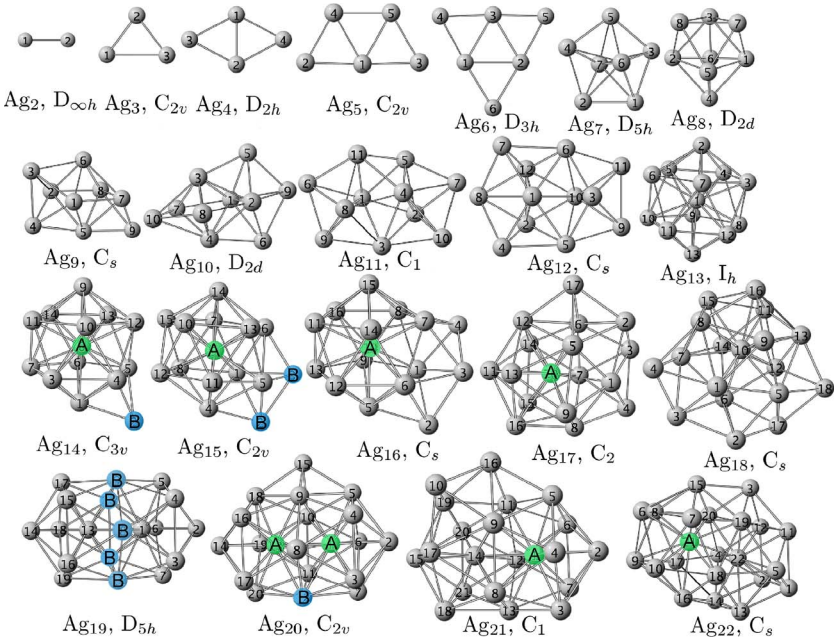

FIG. 1. (Color online) Lowest-energy structures and symmetry point groups assigned to the Ag_n ($2 \leq n \leq 22$) clusters. The magnetic moments, namely, m, of the atoms labeled with the capital letters A ($-1.5\mu_B \leq m \leq -0.4\mu_B$) and B ($-0.1\mu_B \leq m \leq 0\mu_B$) are aligned antiferromagnetically to the other ones.

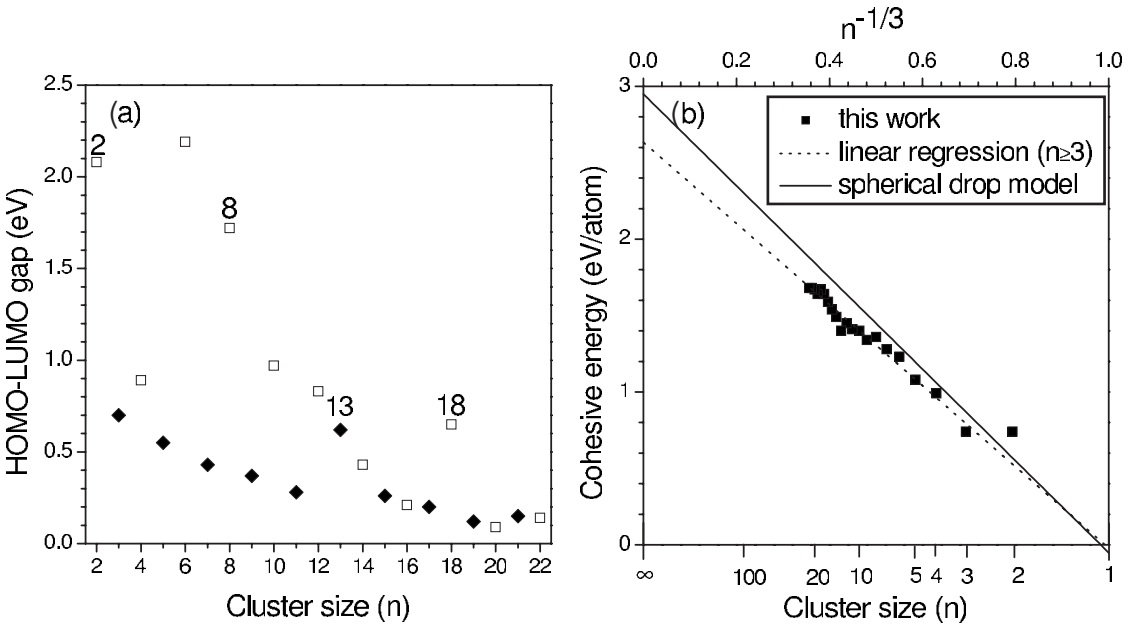

FIG. 2. (a) HOMO-LUMO gap and (b) cohesive energy per atom of small silver clusters as a function of the cluster size n ($2 \leqslant n \leqslant 22$). The empty and filled points represent the even- and odd-numbered clusters, respectively.

III. RESULTS AND DISCUSSION

One of the criteria for a cluster to be used as a potential building block for a nanomaterial is its chemical stability relative to other clusters of the same material. With the aim of studying the stability of Ag_2–Ag_{22} clusters, we have plotted the gaps between the highest occupied (HOMO) and lowest unoccupied (LUMO) molecular orbitals and the cohesive energies in Figs. 2(a) and 2(b), respectively. The cohesive energies for Ag clusters are fitted to a linear regression and compared in Fig. 2(b) with the spherical droplet model of Miedema [17],

$$E_c(n) = E_{bc} - \left(\frac{36\pi}{n}\right)^{1/3} \gamma^0 V_a^{2/3}, \tag{1}$$

where E_{bc} is the bulk cohesive energy, $\gamma^0 = 7.8 \times 10^{18}$ eV/m^2 is the surface energy of the bulk silver, V_a is

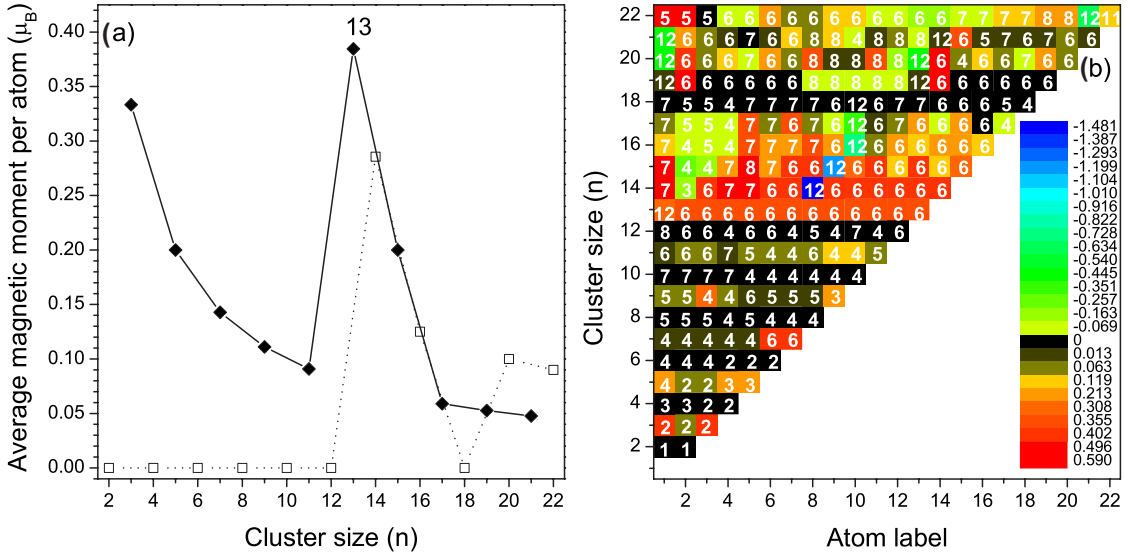

FIG. 3. (Color online) Evolution of magnetic moment per atom of the most stable cluster isomers of each size. (a) Average magnetic moment per atom versus cluster size. The empty and filled points denote the same as in Fig. 2. (b) Color representation of the magnetic moment per atom of each silver cluster. The numbers inside the small charts denote the coordination number. On the right side, the color palette gives information about the numerical values of the atomic magnetic moments. The numbers labeling every atom of each cluster in Fig. 1 are closely related to the ones displayed on the x axis.

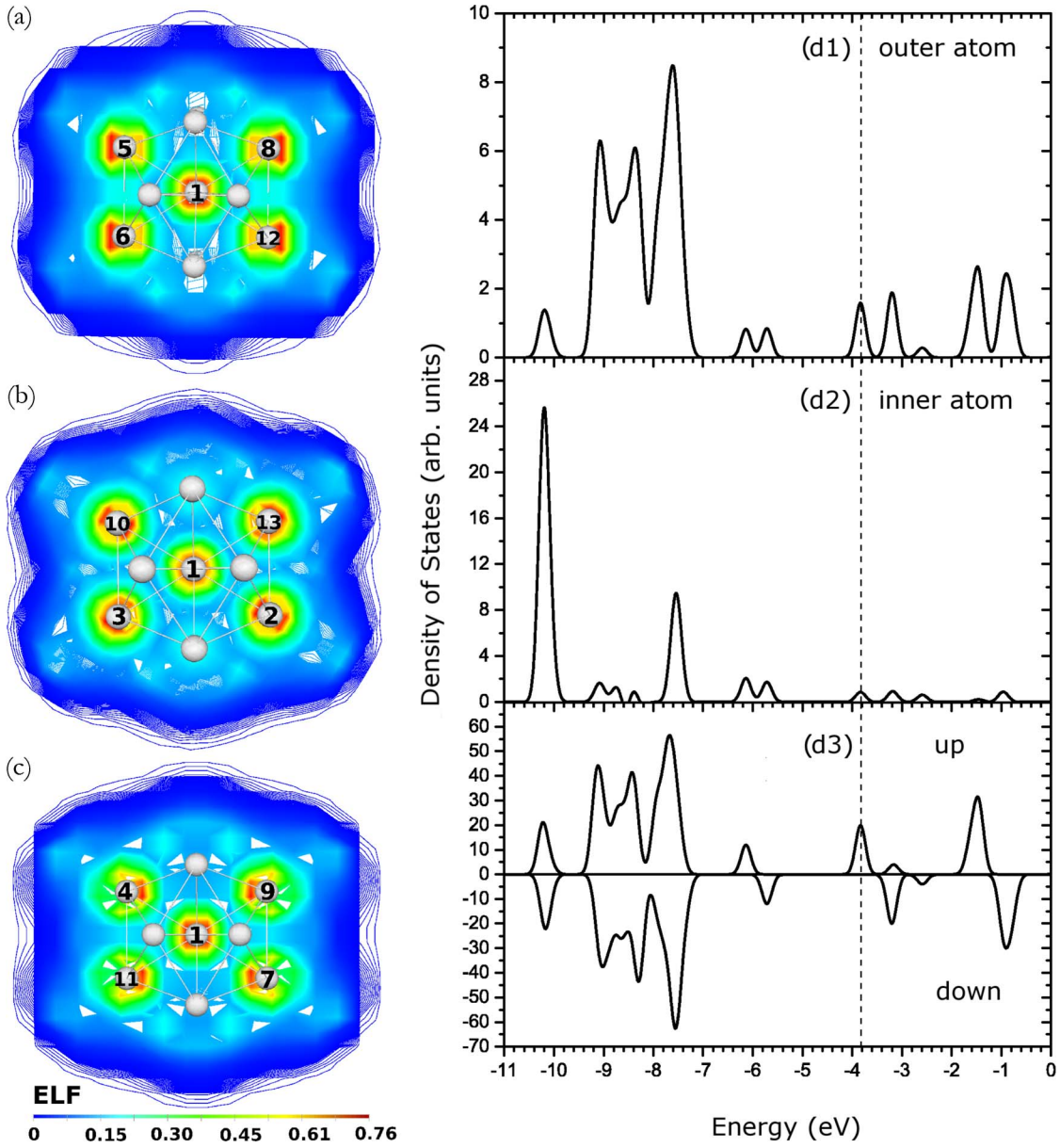

FIG. 4. (Color online) Contour plot of the electron localization function for the three mutually orthogonal golden planes [(a), (b), (c)] of the icosahedral symmetry and densities of states for the outer-shell atoms (d1) and inner atom (d2) in an Ag_{13} cluster. The spin-polarized DOS is shown in (d3). The dashed vertical line represents the Fermi level.

the atomic volume, and n is the number of atoms in the cluster. Despite the fact that some clusters ($2 \leqslant n \leqslant 6$) are far from spherical, our calculated cohesive energies are in good agreement with Miedema's model. Indeed, the bulk cohesive energy predicted by our calculations (2.63 eV/atom) differs by only 10% from the experimental findings (2.95 eV/atom) [18], giving us confidence that the lowest-energy structures plotted in Fig. 1 are reliable. In Fig. 2(a) we can see that the most stable even-numbered clusters are Ag_2, Ag_6, Ag_8, and Ag_{18}. Except for Ag_6, this is a consequence of the closure of the electronic shell [19]. For the odd-numbered clusters, the HOMO-LUMO gaps decrease monotonically as the cluster size increase, except for the Ag_{13} cluster. The large HOMO-LUMO gap of Ag_{13} relative to the odd-numbered clusters enhances its chemical stability and inertness, as well as its ability to assemble into magnetic nanoparticles, because it is a magnetic cluster with a considerable magnetic moment per atom, as is discussed below.

Our results on the magnetic properties of the Ag_n ($2 \leqslant n \leqslant 22$) clusters are most fascinating, if not unexpected, compared with the silver bulk magnetic properties. Indeed, the silver bulk magnetic ordering is well known to be diamagnetic, as can be inferred from its negative magnetic susceptibility ($\chi_m = -19.5 \times 10^{-6}$ cm^3/mol), whereas silver atoms when they coagulate to a cluster become either magnetic or nonmagnetic depending on the cluster size, as is shown in Table I and Fig. 3.

For Ag_2, Ag_8, and Ag_{18} clusters, our calculations clearly show that they are highly stable with large HOMO-LUMO gaps [see Fig. 2(a)] and diamagnetic [see Fig. 3]. The phe-

nomenon can be understood simply from the two-, eight-, and 18-electron rule, as described by the cluster shell models [20]. This rule predicts transition metal clusters to be stable and diamagnetic when the valence shell of the metal atom contains two, eight, or 18 electrons that completely fill electron shells, forming closed electronic structures with paired spins.

From Ag_3 up to Ag_{12} excluding Ag_2 and Ag_8, the cluster topologies converge into a geometry where all atoms belong to the surface (Fig. 1), and consequently have a reduced coordination number [Fig. 3(b)]. This condition favors a reduced charge accumulation in nearest neighbor atoms which according to the calculated Mulliken population analysis (MPA) is less than 0.1 electron per atom in average. Likewise, a Mayer bond order analysis reveals that silver atoms are sharing the unpaired 5*s* electrons, forming a covalent bond, and thereby low-spin configurations are expected. For example, the even-numbered clusters become diamagnetic because they have an even number of 5*s* electrons that create a cloud of paired 5*s* electrons [Fig. 3(a)], whereas for the odd-numbered clusters the electronic configuration with one unpaired spin electron is favored energetically over all the feasible spin configurations studied in this work. The resulting odd-numbered clusters retain an average magnetic moment per atom that decreases monotonically with the increase of the coordination number [Figs. 3(a) and 3(b)] since the orbital overlap expands as the coordination number does, as was reported for Fe, Co, and Ni in Ref. [21] and for 13-atom clusters of Pd, Rh, and Ru in Ref. [7].

In Fig. 3(a) we can see that Ag_{13} exhibits the highest average magnetic moment per atom among the studied clusters. To understand the origin of this considerable magnetic moment ($0.39\mu_B$/atom) we show in Figs. 4(a)–4(d) the electron localization function (ELF) [22] and the densities of states (DOSs) for the inner- and outer-shell atoms. The MPA reveals that the electron charge transfers from the outer-shell Ag atoms to the central Ag atom, which gains an excess of charge of about 0.8 electrons. The charge transfer, which is favored by the icosahedral symmetry, can be described graphically from our corresponding ELF plot. In Figs. 4(a)–4(c), the contour plot of the ELF indicates a slight concentration of the light blue color (0.15–0.30 in the bar color) surrounding the central atom, and gives rise to an enhancement of the electron localization around the inner atom. The large coordination number of the central Ag atom results in an enhancement of the overlap of its 4*d* orbitals with those of other outer-shell Ag atoms. Therefore, for the inner atom the charge transfer populates mainly the lower-energy 4*d* states (~ -10.2 eV) with reduced exchange splitting, whereas for the outer-shell atoms these states become less occupied, as is shown in Figs. 4(d1) and 4(d2) [23], and Fig. 4(d3), respectively. Thereby, the charge transfer lead to a small loss of the spin-up DOS at the Fermi level for the inner atom compared with the outer-shell atoms and, consequently, the inner atom has weaker magnetism ($0.35\mu_B$/atom) and the outer-shell atoms enhance their magnetic moments ($0.39\mu_B$/atom), giving rise to an increase of the average magnetic moment of the Ag_{13} cluster.

From Ag_{14} to Ag_{22}, except for Ag_{18} which has already been studied above, the clusters converge into a distorted icosahedral symmetry in which, depending on the cluster size, the number of inner atoms is either one or two (see Fig. 1). In this case, the MPA confirms a charge transfer mainly from the peripheral atoms to the inner ones even greater than in the Ag_{13} case. This effect decompensates the spin pairing state and gives rise to an antiferromagnetic alignment of the inner atoms to the outer ones, and thus the clusters decrease the total magnetic moment compared with the Ag_{13} cluster, as is shown in Figs. 1 and 3(b). It is also observed in Fig. 3(a) that the average magnetic moment per atom decreases as the cluster size gets bigger up to $n=19$, and then oscillates, tending to decrease. The phenomenon can be understood simply from the loss of symmetry that reduces orbital degeneracy and weakens magnetism [24]. According to this tendency, we expect for clusters greater in size an enhancement of the magnetic moment, as long as the cluster stabilizes in a geometry of high symmetry (e.g., Ag_{55} and Ag_{75}).

IV. SUMMARY

In conclusion, we have shown that the silver atoms can be magnetic when they are grouped together in small clusters. In particular, the Ag_{13} cluster exhibits the highest magnetic moment per atom among the studied silver clusters, due to its high symmetry and degeneracy.

ACKNOWLEDGMENTS

The authors acknowledge the CESGA (Centro de Supercomputación de Galicia), especially A. Gómez and C. Fernández, for computational assistance. The work was supported by the Xunta de Galicia under the Project No. PGIDIT02TMT20601PR.

[1] *Clusters of Atoms and Molecules: Theory, Experiment, and Clusters of Atoms*, edited by H. Haberland (Springer, Berlin, 1994).
[2] C. R. Henry, Surf. Sci. Rep. **31**, 235 (1998).
[3] C. C. Berry and A. S. G. Curtis, J. Phys. D **36**, R198 (2003); Q. A. Pankhurst, J. Connolly, S. K. Jones, and J. Dobson, *ibid.* **36**, R167 (2003); P. Tartaj, M. del Puerto Morales, S. Veintemillas-Verdager, T. González-Carreño, and C. J. Serna, *ibid.* **36**, R182 (2003).
[4] J. A. Alonso, Chem. Rev. (Washington, D.C.) **100**, 637 (2000).
[5] I. M. L. Billas, A. Chatelain, and W. A. de Heer, Science **265**, 1682 (1994).
[6] S. N. Khanna and S. Linderoth, Phys. Rev. Lett. **67**, 742 (1991).
[7] B. V. Reddy, S. N. Khanna, and B. I. Dunlap, Phys. Rev. Lett. **70**, 3323 (1993).

[8] A. St-Amant and D. R. Salahub, Chem. Phys. Lett. **169**, 387 (1990).
[9] J. P. Perdew and Y. Wang, Phys. Rev. B **46**, 12947 (1992).
[10] M. Pereiro, D. Baldomir, M. Iglesias, C. Rosales, and M. Castro, Int. J. Quantum Chem. **81**, 422 (2001).
[11] B. Simard, P. A. Hackett, A. M. James, and P. R. R. Langridge-Smith, Chem. Phys. Lett. **186**, 415 (1991).
[12] S. Huzinaga, J. Andzelm, M. Klobukowski, E. Radzio-Andzelm, Y. Sakai, and H. Tatewaki, *Gaussian Basis Sets for Molecular Calculations* (Elsevier, Amsterdam, 1984).
[13] L. Versluis and T. Ziegler, J. Chem. Phys. **88**, 322 (1988).
[14] H. B. Schlegel, *Modern Electronic Structure Theory* (World Scientific, Singapore, 1995), Chap. 8, p. 459.
[15] M. Pereiro and D. Baldomir, Phys. Rev. A **75**, 033202 (2007).
[16] E. M. Fernández, J. M. Soler, I. L. Garzón, and L. C. Balbás, Phys. Rev. B **70**, 165403 (2004).
[17] A. R. Miedema, Z. Metallkd. **69**, 287 (1978).
[18] C. Kittel, *Introduction to Solid State Physics*, 8th ed. (Wiley, New York, 2005).
[19] M. Pereiro and D. Baldomir, Phys. Rev. A **72**, 045201 (2005).
[20] R. H. Crabtree, *The Organometallic Chemistry of the Transition Metals* (Wiley, New York, 1988).
[21] F. Liu, M. R. Press, S. N. Khanna, and P. Jena, Phys. Rev. B **39**, 6914 (1989).
[22] A. D. Becke and K. E. Edgecombe, J. Chem. Phys. **92**, 5397 (1990).
[23] In Fig. 4(d1), we show the DOS for the atom labeled with the number 2 in Fig. 1 as a representative example of the DOSs for the outer-shell atoms, since from symmetry considerations the external atoms have all similar DOS plots.
[24] B. I. Dunlap, Phys. Rev. A **41**, 5691 (1990).